Electronic Research Archive

https://www.aimspress.com/journal/era

ERA, 34(10): 7222–7243.
DOI: 10.3934/era.2026312
Received: 06 July 2026
Revised: 07 August 2026
Accepted: 10 August 2026
Published: 18 August 2026

Research article

Cooperative pointing control of multi-agent systems with switching topologies via distributed error estimation

Cui-Li Jin[1], **Yuhai Yang**[2], **Bing Tan**[3,*] **and Jinlong Yuan**[4,*]

[1] College of Marine Electrical Engineering, Dalian Maritime University, Dalian 116026, China
[2] Dalian Kerun Intelligent Technology Co., Ltd, Dalian 116023, China
[3] School of Mathematics and Statistics, Nanyang Normal University, Nanyang 473061, China
[4] School of Science, Dalian Maritime University, Dalian 116026, China

* **Correspondence:** Email: tanbing@nynu.edu.cn, yuanjinlong@dlmu.edu.cn.

Abstract: This paper proposes a distributed relative-position-based cooperative pointing control scheme for stationary planar multi-agent systems toward a stationary target under switching topologies. First, the proposed scheme only requires the leaders' orientation angles and relative position measurements, without relying on the agents' states in a common global coordinate frame. Then, the cooperative control problem is decoupled into cooperative target localization and local pointing control. In the proposed scheme, the cooperative target localization problem is modeled as a distributed relative position estimation system, in which the system dynamics are determined by the switching topologies and the projection matrices induced by the leaders' orientation angles. Under minimal information conditions, sufficient conditions are established to ensure the convergence of the proposed scheme by developing a novel error estimator and multiple Lyapunov functions. As a result, the generated reference orientations converge to the desired ones, and the local pointing controllers track them asymptotically. Finally, numerical simulations validate the effectiveness of the proposed method.

Keywords: multi-agent systems; switching topologies; cooperative control; pointing control; distributed estimation

1. Introduction

The cooperative pointing control of multi-agent systems aims to orchestrate multiple agents so that their pointing lines (or lines of sight) simultaneously converge on a common target. This capability is critical in many practical tasks [1–5]. For example, satellite formations must synchronously gaze at a specific region of the earth from different viewpoints to estimate the reflected energy [3]. Unmanned aerial vehicle swarms rely on multi-angle cooperative observations to overcome line-of-sight obstructions in forests or disaster areas, thereby enabling the detection and tracking of concealed targets [4, 5]. Unlike classical distributed attitude alignment problems such as those studied in [6, 7], cooperative pointing control requires agents to jointly infer the unknown target position through local information exchange rather than merely aligning their own orientation with others, thereby driving all pointing lines to precisely intersect at the target point.

In [8], a simplified scenario of cooperative pointing control is considered, where collinear agents are arranged in a linear array, with the two end agents already pre-pointed toward the target. The middle agents adjust the heights of the intersections between their own half-lines directed toward the target and those of their left and right neighbors. Utilizing an adjacent interaction protocol, they equalize all these heights, thereby achieving collective convergence without prior knowledge of the target coordinates. The height equalization strategy in [8] was extended to a three-dimensional space in [9] via an update protocol. This protocol ensures that distances, measured relative to a reference line defined by the intersection points of adjacent half-lines projected onto a reference plane, remain consistent. The collinearity constraint in [8–10] was relaxed to coplanarity in [11], with agents deployed on a single plane and the target outside it. However, since it lacks the strict collinearity condition, this work introduces a decoupling approach that splits the three-dimensional pointing task into two independent planar projections. Then, by adjusting the positional difference between the intersection points of adjacent half-lines on each projected plane, the system guides all half-lines to converge at the target. [12] further relaxed constraints on agent spatial arrangements by applying the geometric invariance of bearing vectors under translation and scaling transformations, which enables agents to orient towards a target point characterized as an invariant set of coordinates under these transformations, without needing to know their absolute positions. It is worth noting that, despite the conservatism in the assumed conditions (such as control strategies, algorithm design, time step selection, and initial conditions), [12] clearly revealed the geometric essence of the cooperative pointing problem: collaborative pointing essentially only requires the pointing line of each agent to converge at the target point in space, without the need for precise estimation and positioning of the target point's absolute coordinates. Unlike the geometric constraints imposed on the entire multi-agent system in [8–12], [13, 14] only required the non-collinearity of the two leaders with the target. Then, [13] adopted a decoupling method similar to that in [12] by decomposing cooperative pointing control into localization estimation and pointing control. The localization estimation was formulated as a switched model for the multi-robot system to avoid potential singularities in pointing control without imposing geometric constraints on the entire system, thereby enhancing the flexibility of agent arrangements. However, the aforementioned results typically assume a time-invariant network topology. This assumption, while simplifying the analysis, significantly deviates from practical scenarios. In fact, in mobile communication networks, drone swarms, and intelligent transportation systems, the connectivity between agents is inherently dynamic. For instance, signal propagation paths can be obstructed by environmental factors, and communication links can be interrupted by packet loss, which directly impacts the agents' communication status. Consequently, the network connectivity is almost always in flux [15–20], rendering a fixed topology merely an idealization. Motivated by this, this paper investigates the cooperative pointing control for multi-agent systems with switching topologies, based exclusively on orientation angles.

This paper addresses the cooperative pointing control of stationary planar multi-agent systems that aim to align with a stationary target under time-varying topologies. First, unlike methods that rely on absolute coordinates and direct distance measurements, this work solely derives control conditions from an undirected connected topology and the agents' observed bearing angles, while relaxing the geometric constraint to the non-collinearity of the two leaders and the target. Then, the cooperative pointing control problem is decoupled into cooperative target localization and local pointing control. The cooperative target localization problem is formulated by introducing orientation-angle-dependent projection matrices. These matrices ensure that the leaders' lines of sight to the target remain aligned, thereby enabling the estimated relative positions to converge to the relative positions between each agent and the target. Next, an error estimator is proposed to overcome the technical difficulties which arise from projection-matrix semidefiniteness and time-varying topologies. Subsequently, multiple Lyapunov functions are designed to analyze its dynamics, thereby rigorously establishing the convergence of the relative-position estimation system. Furthermore, the local pointing control ensures asymptotic tracking of the orientation angles provided by the target localization process, while the resulting localization estimate itself converges to the target. Finally, numerical simulations validate the effectiveness of the proposed strategy, thereby showing that it can achieve cooperative pointing control without requiring absolute coordinate information or direct distance measurements to the target.

The main contributions of this paper are summarized as follows. (1) A distributed relative-position -based estimation framework is proposed for the cooperative pointing control of planar multi-agent systems under switching communication topologies. The proposed framework only requires the leaders' orientation angles and relative position measurements, without requiring the agents' states to be expressed in a common global coordinate frame. (2) This paper addresses a nontrivial extension from fixed communication graphs to switching topologies. Unlike existing studies, the resulting closed-loop system simultaneously involves state-dependent switching induced by geometric constraints and topology-dependent switching induced by time-varying communication graphs. (3) To handle these difficulties, a novel error estimator and a Lyapunov-based analysis are developed. Under relatively mild conditions, sufficient admissibility conditions are established to guarantee the convergence of the proposed scheme.

Notation: $\mathbb{N}$ and $\mathbb{N}^+$ denote the set of non-negative and positive integers. $\mathbb{R}^n$ and $\mathbb{R}^{n\times m}$ denote the set of n-dimensional column vectors and $n\times m$ real matrices, respectively. $M_1 \otimes M_2$ denotes the Kronecker product of matrices M_1 and M_2. $\mathbf{I}_n$ denotes the $n \times n$ identity matrix. $\mathbf{1}_n$ denotes a n-dimensional vector of all ones. $\mathbf{0}$ denotes a zero matrix of appropriate dimensionality. $\|\cdot\|$ denotes the operator that computes the Euclidean vector or matrix norm. $\mathrm{bkdg}\{M_1, M_2, \ldots, M_N\}$ denotes the operator that forms a block diagonal matrix with diagonal entries $M_1, M_2, \ldots, M_N$. $\lambda^+_{\min}(M)$ and $\lambda_{\max}(M)$ denote the operators that compute the smallest positive eigenvalue and the largest positive eigenvalue of the matrix M, respectively.

2. Problem formulation

This paper considers a swarm of N agents ($N > 2$) arbitrarily deployed within the common 0-X-Y plane, as depicted in Figure 1. The position of each agent in the global coordinate frame 0-X-Y is marked as $p_i = [x_i, y_i]^T \in \mathbb{R}^2$. Its orientation angle $\theta_i \in [0, 2\pi)$ is, measured counterclockwise from the positive X_i-axis of the local coordinate frame p_i-X_i-Y_i, which is defined with its origin at p_i and axes X_i and Y_i. The local coordinate frames share the same orientation as the global coordinate frame, but their origins are offset. These N agents, each equipped with its own local coordinate frame, exchange information with their neighbors over an undirected, connected, and time-varying communication graph $\mathcal{G}_t \in \{\mathcal{G}_1, \mathcal{G}_2, \ldots, \mathcal{G}_g\}$. The Laplacian matrix of $\mathcal{G}_t$ at time t is formally defined as $L_{\sigma(t)}$, where $\sigma(\cdot) : [0, +\infty) \to N_g = \{1, 2, \ldots, g\}$ is the discrete logical signal orchestrating the switching between topologies, and L_j represents the Laplacian matrix of the topology graph $\mathcal{G}_j$ for $j \in N_g$. The switching signal $\sigma(t)$ defines a switching sequence $\{(\sigma(t_0), t_0), \ldots, (\sigma(t_h), t_h) | h = 1, 2, \ldots\}$, where $(\sigma(t_h), t_h)$ means that the $\sigma(t_h)$-th topology graph $\mathcal{G}_{\sigma(t_h)}$ is activated during $t \in [t_h, t_{h+1})$.

Definition 1. *For any $T_2 > T_1 \geq 0$, let $N_\sigma(T_1, T_2)$ denote the number of switching of $\sigma(t)$ over (T_1, T_2). If $N_\sigma(T_1, T_2) \leq N_0 + (T_2 - T_1)/\tau_{ave}$ holds for $\tau_{ave} > 0$, $N_0 \geq 0$, then τ_{ave} is called the average dwell time. As commonly used in the literature, we choose $N_0 = 0$.*

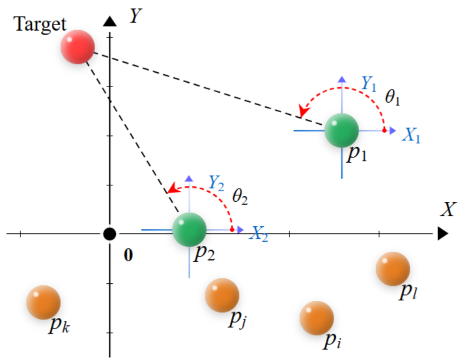

Figure 1. A diagram of cooperative pointing control.

The collaborative task is to drive all agents through communication to orient towards the target, whose position in the global coordinate frame is marked by $q = [x, y]^T \in \mathbb{R}^2$, where only agents $i = 1, 2$ possess the capability to measure their orientation angle θ_i towards the target, known from the outset. Then, based on the rotating dynamics system

$$\dot{\theta}_i(t) = u_i(t), \ \ i = 1, 2, ..., N, \tag{2.1}$$

the cooperative pointing control problem is stated as designing the control input u_i such that θ_i converges to θ_i^*, which means driving the orientation half-lines of all the robots to point to the target, where

$$\theta_i^* = \begin{cases} \arccos \frac{x - x_i}{\|d_i\|}, & \text{if } y - y_i \geq 0 \\ 2\pi - \arccos \frac{x - x_i}{\|d_i\|}, & \text{otherwise} \end{cases},$$

and $d_i = q - p_i$, $i \in \{1, 2, \ldots, N\}$. It is worth emphasizing that q is not known to agent i, and thus θ_i^* is unknown in advance either. However, Agents 1 and 2 are allowed to obtain their orientations to the target, and they simply hold them (i.e., $u_1(t) \equiv 0$ and $u_2(t) \equiv 0$), indicating that $\theta_1(t) \equiv \theta_1(t_0) \equiv \theta_1^*$ and $\theta_2(t) \equiv \theta_2(t_0) \equiv \theta_2^*$.

Throughout the paper, it is assumed that Agents 1 and 2, called leader agents, and the target are not collinear, so that the target directional information obtained by Agents 1 and 2 uniquely identifies the target, and this assumption is stated as follows.

Assumption 1 [13]**.** *$\theta_1 \neq \theta_2$ and $\theta_1 \neq \theta_2 \pm \pi$.*

Moreover, the following lemmas are also needed.

Lemma 1. *Let $K_F = \mathrm{bkdg}\{\zeta_1^T, \zeta_2^T, \underbrace{\mathbf{I}_2, \ldots, \mathbf{I}_2}_{N-2}\} \in \mathbb{R}^{(2N-2)\times 2N}$, $F_{\sigma(t)} = K_F(L_{\sigma(t)} \otimes \mathbf{I}_2)(K_F)^T$, where $\zeta_1 = [\cos\theta_1, \sin\theta_1]^T$ and $\zeta_2 = [\cos\theta_2, \sin\theta_2]^T$. Then, under Assumption 1, the following inequality holds:*

$$0 < \lambda_{\min,F} = \min_{i\in N_g}\{\lambda_{\min}(F_i)\} \leq C_{\min}\sin^2(\theta_1 - \theta_2), \tag{2.2}$$

where $C_{\min} = \min_{i\in N_g}\{\mathrm{e}_2^T L_i \mathrm{e}_2\}$, and $e_2 = [0, 1, 0, \ldots, 0]^T$.

Proof. Let $\triangle\theta = \theta_1 - \theta_2$, $\eta = [1, \cos(\triangle\theta), \underbrace{\zeta_1^T, \ldots, \zeta_1^T}_{N-2}]^T \in \mathbb{R}^{2N-2}$. Then,

$$K_F^T\eta = [\zeta_1^T, (\cos(\triangle\theta)\zeta_2)^T, \zeta_1^T, \ldots, \zeta_1^T]^T = \mathbf{1}_N \otimes \zeta_1 + \mathrm{e}_2 \otimes (\cos(\triangle\theta)\zeta_2 - \zeta_1),$$

and

$$\|\eta\|^2 = 1 + \cos^2(\triangle\theta) + (N-2) = N - 1 + \cos^2(\triangle\theta) \geq 1.$$

Given that $\|\zeta_1\| = \|\zeta_2\| = 1$, the squared norm of $\cos(\triangle\theta)\zeta_2 - \zeta_1$ is $\|\cos(\triangle\theta)\zeta_2 - \zeta_1\|^2 = \cos^2(\triangle\theta)\|\zeta_2\|^2 + \|\zeta_1\|^2 - 2\cos(\triangle\theta)(\zeta_2^T\zeta_1) = \cos^2(\triangle\theta) + 1 - 2\cos^2(\triangle\theta) = \sin^2(\triangle\theta)$. Since $L_{\sigma(t)}\mathbf{1}_N = \mathbf{1}_N^T L_{\sigma(t)} = 0$, it follows that

$$\begin{aligned}
\eta^T F_{\sigma(t)}\eta &= \eta^T K_F(L_{\sigma(t)} \otimes \mathbf{I}_2)K_F^T\eta \\
&= (\mathrm{e}_2 \otimes (\cos(\triangle\theta)\zeta_2 - \zeta_1))^T (L_{\sigma(t)} \otimes \mathbf{I}_2)(\mathrm{e}_2 \otimes (\cos(\triangle\theta)\zeta_2 - \zeta_1)) \\
&= (\mathrm{e}_2^T L_{\sigma(t)}\mathrm{e}_2)((\cos(\triangle\theta)\zeta_2 - \zeta_1)\mathbf{I}_2(\cos(\triangle\theta)\zeta_2 - \zeta_1)) \\
&= (\mathrm{e}_2^T L_{\sigma(t)}\mathrm{e}_2)\|\cos(\triangle\theta)\zeta_2 - \zeta_1\|^2 \\
&= (\mathrm{e}_2^T L_{\sigma(t)}\mathrm{e}_2)\sin^2(\triangle\theta).
\end{aligned}$$

Therefore, the minimum eigenvalue of $F_{\sigma(t)}$ satisfies the following:

$$\lambda_{\min}(F_{\sigma(t)}) \leq \frac{\eta^T F_{\sigma(t)}\eta}{\eta^T\eta} = \frac{(\mathrm{e}_2^T L_{\sigma(t)}\mathrm{e}_2)\sin^2(\triangle\theta)}{N - 1 + \cos^2(\triangle\theta)} \leq \mathrm{e}_2^T L_{\sigma(t)}\mathrm{e}_2 \sin^2(\triangle\theta).$$

This implies that $\min_{i\in N_g}\{\lambda_{\min}(F_i)\} \leq C_{\min}\sin^2(\theta_1 - \theta_2)$. On the other hand, for any $i \in N_g$, suppose there exists a non-zero vector $\eta = [\eta_1, \eta_2, \eta_3^T, \ldots, \eta_N^T]^T \in \mathbb{R}^{2N-2}$ such that $\eta^T F_i \eta = 0$, where $\eta_1, \eta_2 \in \mathbb{R}$, and $\eta_3 \in \mathbb{R}^2$ for $i = 3, \ldots, N$. Then, $(K_F^T\eta)^T(L_{\sigma(t)} \otimes \mathbf{I}_2)K_F^T\eta = 0$. This means

$$K_F^T\eta = [\eta_1\zeta_1^T, \eta_2\zeta_2^T, \eta_3^T, \ldots, \eta_N^T]^T = \mathbf{1}_N \otimes \eta_0$$

holds for some $\eta_0 \in \mathbb{R}^2$. This further implies $\eta_1\zeta_1 = \eta_2\zeta_2 = \eta_i = \eta_0$, for $i = 3, 4, \ldots, N$. Given that $\theta_1 \neq \theta_2$ and $\theta_1 \neq \theta_2 \pm \pi$, the equality $\eta_1\zeta_1 = \eta_2\zeta_2$ implies $\eta_1 = \eta_2 = 0$. Consequently, $\eta_0 = \mathbf{0}$, which contradicts the initial assumption that $\eta \neq \mathbf{0}$. Therefore, it must be that $0 < \lambda_{\min,F}$. This concludes the proof. ◻

Lemma 2. *Let L be the Laplacian matrix of a connected undirected graph with n vertices, and $X \in \mathbb{R}^{2n\times 2n}$ be a real symmetric positive semi-definite matrix that satisfies the following:*

$$\mathrm{Ker}(X) \cap \mathrm{Im}(L \otimes \mathbf{I}_2) = \{\mathbf{0}\}.$$

Then, for every vector $\eta \in \mathbb{R}^{2N}$ *such that* $(\mathbf{1}_N^T \otimes \mathbf{I}_2)\eta = \mathbf{0}$*, it holds that*

$$\lambda_{\min}^{+}(M)\eta^T\eta \leq \eta^T M\eta \leq \lambda_{\max}(M)\eta^T\eta,$$

where $M = (L \otimes \mathbf{I}_2)X(L \otimes \mathbf{I}_2)$.

Proof. Let $Y = (L \otimes \mathbf{I}_2)$. Since X is positive semi-definite, then for any $\eta \in \mathbb{R}^{2N}$,

$$\eta^T M\eta = (Y\eta)^T X(Y\eta) \geq 0.$$

This implies

$$\eta^T M\eta = 0 \iff M\eta = \mathbf{0} \iff \eta \in \mathrm{Ker}(M),$$

and

$$(Y\eta)^T X(Y\eta) = 0 \iff X(Y\eta) = \mathbf{0} \iff Y\eta \in \mathrm{Ker}(X).$$

It is obvious that $Y\eta \in \mathrm{Im}(Y)$ always holds, which indicates that

$$\eta^T M\eta = 0 \iff (Y\eta) \in \mathrm{Ker}(X) \cap \mathrm{Im}(Y).$$

By the known condition $\mathrm{Ker}(X) \cap \mathrm{Im}(Y) = \{\mathbf{0}\}$, it follows that

$$\eta^T M\eta = 0 \iff (Y\eta) = \mathbf{0} \iff \eta \in \mathrm{Ker}(Y).$$

Thus, $\mathrm{Ker}(M) = \mathrm{Ker}(Y)$. The graph is connected, $\mathrm{Ker}(L) = \mathrm{span}\{\mathbf{1}_N\}$(i.e., the one-dimensional subspace spanned by the all-ones vector). Hence, $\mathrm{Ker}(M) = \mathrm{Ker}(Y) = \mathrm{Ker}(L \otimes \mathbf{I}_2) = \{\mathbf{1}_N \otimes w : w \in \mathbb{R}^2\}$ and $\dim(\mathrm{Ker}(M)) = 2$.

Write η as $\eta = (\eta_1^T, \eta_2^T, \ldots, \eta_N^T)^T$ with each $\eta_i \in \mathbb{R}^2$. Then, $(\mathbf{1}_N^T \otimes \mathbf{I}_2)\eta = \sum_{i=1}^N \eta_i$, and consequently, $(\mathbf{1}_N^T \otimes \mathbf{I}_2)\eta = \mathbf{0}$ is equivalent to $\sum_{i=1}^N \eta_i = \mathbf{0}$. For any $w \in \mathbb{R}^2$, it holds that $(\mathbf{1}_N \otimes w)^T\eta = w^T \sum_{i=1}^N \eta_i$. If $(\mathbf{1}_N^T \otimes \mathbf{I}_2)\eta = \mathbf{0}$ (i.e., $\sum_{i=1}^N \eta_i = \mathbf{0}$), then $(\mathbf{1}_N \otimes w)^T\eta = \mathbf{0}$ for every w, hence $\eta \perp \mathrm{Ker}(M)$. Conversely, suppose $\eta \perp \mathrm{Ker}(M)$. This implies $w^T \sum_{i=1}^N \eta_i = 0$ for all $w \in \mathbb{R}^2$. Choosing $w = w_1 = [1, 0]^T$ and $w = w_2 = [0, 1]^T$ yields $w_1^T \sum_{i=1}^N \eta_i = 0$ and $w_2^T \sum_{i=1}^N \eta_i = 0$, which together force $\sum_{i=1}^N \eta_i = 0$. Therefore,

$$(\mathbf{1}_N^T \otimes \mathbf{I}_2)\eta = 0 \iff \eta \perp \mathrm{Ker}(M).$$

Because M is real symmetric positive semi-definite, there exists a set of orthogonal eigenvectors $\{w_1, w_2, \ldots, w_{2N}\}$ with corresponding eigenvalues satisfying $0 = \lambda_1 = \lambda_2 < \lambda_3 \leq \lambda_4 \leq \cdots \leq \lambda_{2N}$, where $w_1, w_2 \in \mathrm{Ker}(M)$, $\lambda_3 = \lambda_{\min}^{+}(M)$, $\lambda_{2N} = \lambda_{\max}(M)$, and

$$w_i^T w_j = \begin{cases} 1, & \text{if } i = j \\ 0, & \text{otherwise} \end{cases}.$$

Consequently, if $\eta \perp \mathrm{Ker}(M)$, then there exist coefficients $c_1, c_2, c_3, \ldots, c_{2N}$ such that $\eta = \sum_{i=1}^{2N} c_i w_i$ with $c_i = w_i^T\eta$ and $c_1 = c_2 = 0$. Next, $\eta^T\eta = \sum_{i=3}^{2N} c_i^2$, and because $Mw_i = \lambda_i w_i$, one obtains $\eta^T M\eta = \sum_{i=3}^{2N} \lambda_i c_i^2$. Since $\lambda_3 \leq \lambda_i \leq \lambda_{2N}$ for all $i \geq 3$, it follows that $\lambda_3 \sum_{i=3}^{2N} c_i^2 \leq \sum_{i=3}^{2N} \lambda_i c_i^2 \leq \lambda_{2N} \sum_{i=3}^{2N} c_i^2$. Substituting the expressions for $\eta^T\eta$ and $\eta^T M\eta$ yields $\lambda_{\min}^{+}(M)\eta^T\eta \leq \eta^T M\eta \leq \lambda_{\max}(M)\eta^T\eta$. This completes the proof. □

3. Cooperative control protocol

This section presents a distributed relative position estimation algorithm for a multi-agent system with a time-varying topology in which only two leader agents possess information about the direction towards the target. The algorithm embeds local orientation information and employs a projection matrix to strictly constrain each leader's estimate updates along the line pointing toward the target. By preserving critical orientation information within the communication network, the algorithm drives the entire network in acquiring relative position estimates of the target for each agent. Further details are provided below.

Consider a distributed relative position estimator with the following structure

$$\dot{\hat{d}}_i(t) = -K_i \sum_{j\in\mathcal{N}_i} a_{\sigma(t),i,j}(\hat{d}_i(t) - d_{i,j} - \hat{d}_j(t)), \tag{3.1}$$

where $\hat{d}_i(t)$ is the estimation of d_i, $d_{i,j} = p_j - p_i$ denotes a relative position vector expressed in a shared global frame, $\mathcal{A}_t = [a_{\sigma(t),i,j}(t)]_{N\times N}$ is the adjacency matrix based on the undirected connected graph $\mathcal{G}_t$ and $\mathcal{N}_i$ is the neighbor set of agent i. The control gain K_i is designed following the method in reference [13], with the specific form as follows:

$$K_i = \begin{cases} \begin{bmatrix} \cos^2\theta_i & \cos\theta_i\sin\theta_i \\ \cos\theta_i\sin\theta_i & \sin^2\theta_i \end{bmatrix}, & \text{if } i = 1,2 \\ \mathbf{I}_2, & \text{otherwise} \end{cases}.$$

It is clear that $d_{i,j} = -d_{j,i}$ because $d_{i,j} = p_j - p_i$ and $d_{j,i} = p_i - p_j$. Thus, $d_j - d_i = q - p_j - (q - p_i) = -(p_j - p_i) = -d_{i,j} = d_{j,i}$, and the compact form of Eq (3.1) can be written as follows:

$$\dot{\hat{d}}(t) = -K(L_{\sigma(t)} \otimes \mathbf{I}_2)\hat{d}(t) - K(L_{\sigma(t)} \otimes \mathbf{I}_2)p, \tag{3.2}$$

where $\hat{d} = [\hat{d}_1^T, \hat{d}_2^T, \ldots, \hat{d}_N^T]^T$, $p = [p_1^T, p_2^T, \ldots, p_N^T]^T$.

Remark 1. *Unlike the algorithm provided in Theorem 1 of reference [13], which depends on a given radius r and whose computation requires global positional information, the estimator given by Eq* (3.2) *is designed to only utilize relative information. For each* $\hat{d}_i$*, its update is based on* $a_{\sigma(t),i,j}(\hat{d}_i(t) - d_{i,j} - \hat{d}_j(t)) = a_{\sigma(t),i,j}(\hat{d}_i(t) - \hat{d}_j(t)) + a_{\sigma(t),i,j}d_{i,j}$*, where* $\hat{d}_i(t) - \hat{d}_j(t)$ *and* $d_{i,j}$ *represent relative information. The compact form in Eq* (3.2) *provides a clearer illustration through the Laplace matrix L.*

Before analyzing the convergence of the relative position estimation algorithm, the following assumptions regarding its initial conditions are required.

Assumption 2. *Assume that for* $i = 1,2$, $\hat{d}_i(t_0)$ *is parallel to the vector* $\overrightarrow{p_i q}$*, i.e.,* $\hat{d}_i(t_0) := \hat{\ell}_i[\cos\theta_i, \sin\theta_i]^T$*, where* $\hat{\ell}_i \in \mathbb{R}/\{0\}$.

Remark 2. *Assumption 2 is an important prerequisite for the effectiveness of the distributed relative position estimator that is formulated in Eq* (3.2)*. Owing to the absence of distance measurements, the leaders' estimates of the target's relative-position vector must be confined to the correct direction to avoid divergence from the true value. The projection matrix ensures that the relative position vector is always parallel to the initial value, so the selection of the initial value must comply with the above assumption.*

Let $e_i(t) = \hat{d}_i(t) - d_i$. This error term drives the following distributed error estimator:

$$\begin{aligned}\dot{e}_i(t) = \dot{\hat{d}}_i(t) &= -K_i \sum_{j\in\mathcal{N}_i} a_{\sigma(t),i,j}(\hat{d}_i(t) - d_{i,j} - \hat{d}_j(t)) \\ &= -K_i \sum_{j\in\mathcal{N}_i} a_{\sigma(t),i,j}(\hat{d}_i(t) - d_i - \hat{d}_j(t) + d_j) \\ &= -K_i \sum_{j\in\mathcal{N}_i} a_{\sigma(t),i,j}(e_i(t) - e_j(t)).\end{aligned}$$

This equation can be expressed in a compact form as follows:

$$\dot{e}(t) = -K(L_{\sigma(t)} \otimes \mathbf{I}_2)e(t), \tag{3.3}$$

where $K = \text{bkdg}\{K_1, K_2, \underbrace{\mathbf{I}_2, \cdots, \mathbf{I}_2}_{N-2}\}$ is positive semi-definite. Then, $\lim_{t\to+\infty} \hat{d}(t) = d$ if $\lim_{t\to+\infty} e(t) = \mathbf{0}$, where $d = [d_1^T, d_2^T, \ldots, d_N^T]^T$.

Furthermore, let

$$\delta = \mathbf{P}e, \tag{3.4}$$

where $\mathbf{P} = \mathbf{I}_{2N} - \frac{1}{N}(\mathbf{1}_N \otimes \mathbf{I}_2)(\mathbf{1}_N^T \otimes \mathbf{I}_2)$, then

$$\delta = e - (\mathbf{1}_N \otimes \mathbf{I}_2)\bar{e}, \tag{3.5}$$

and

$$\begin{aligned}(\mathbf{1}_N^T \otimes \mathbf{I}_2)\delta &= (\mathbf{1}_N^T \otimes \mathbf{I}_2)\left[e - \frac{1}{N}(\mathbf{1}_N \otimes \mathbf{I}_2)(\mathbf{1}_N^T \otimes \mathbf{I}_2)e\right] \\ &= (\mathbf{1}_N^T \otimes \mathbf{I}_2)e - \frac{1}{N}(\mathbf{1}_N^T \otimes \mathbf{I}_2)(\mathbf{1}_N \otimes \mathbf{I}_2)(\mathbf{1}_N^T \otimes \mathbf{I}_2)e \\ &= (\mathbf{1}_N^T \otimes \mathbf{I}_2)e - \frac{1}{N}\left[(\mathbf{1}_N^T\mathbf{1}_N) \otimes \mathbf{I}_2\right](\mathbf{1}_N^T \otimes \mathbf{I}_2)e \\ &= (\mathbf{1}_N^T \otimes \mathbf{I}_2)e - \mathbf{I}_2(\mathbf{1}_N^T \otimes \mathbf{I}_2)e \\ &= \mathbf{0},\end{aligned}$$

where $\bar{e} = \frac{1}{N}(\mathbf{1}_N^T \otimes \mathbf{I}_2)e \in \mathbb{R}^2$. Write δ as $\delta = (\delta_1^T, \delta_2^T, \ldots, \delta_N^T)^T$ with each $\delta_i \in \mathbb{R}^2$. Then, $\delta_i = e_i - \bar{e}$ holds, following Eq (3.5), which indicates that

$$e_i - e_j = \delta_i - \delta_j. \tag{3.6}$$

It follows that, $\delta_i = \delta_j$ if and only if $e_i = e_j$. Combining Eqs (3.3)–(3.5) yields the following:

$$\dot{\delta} = \mathbf{P}\dot{e} = -\mathbf{P}K(L_{\sigma(t)} \otimes \mathbf{I}_2)e = -\mathbf{P}K(L_{\sigma(t)} \otimes \mathbf{I}_2)\left[\delta + (\mathbf{1}_N \otimes \mathbf{I}_2)\bar{e}\right] = -\mathbf{P}K(L_{\sigma(t)} \otimes \mathbf{I}_2)\delta. \tag{3.7}$$

Remark 3. *Note that*

$$\mathbf{P} = \mathbf{I}_{2N} - \frac{1}{N}(\mathbf{1}_N \otimes \mathbf{I}_2)(\mathbf{1}_N^T \otimes \mathbf{I}_2) = \mathbf{I}_{2N} - \frac{1}{N}(\mathbf{1}_N\mathbf{1}_N^T) \otimes \mathbf{I}_2 = \left(\mathbf{I}_N - \frac{1}{N}\mathbf{1}_N\mathbf{1}_N^T\right) \otimes \mathbf{I}_2.$$

Since $L_{\sigma(t)}\mathbf{1}_N = 0$*, it follows that*

$$L_{\sigma(t)}\mathbf{1}_N\mathbf{1}_N^T = 0,$$

which implies

$$(L_{\sigma(t)}\otimes \mathbf{I}_2)\mathbf{P} = (L_{\sigma(t)}\otimes \mathbf{I}_2)\left[\left(\mathbf{I}_N - \frac{1}{N}\mathbf{1}_N\mathbf{1}_N^T\right)\otimes \mathbf{I}_2\right] = \left[L_{\sigma(t)}\left(\mathbf{I}_N - \frac{1}{N}\mathbf{1}_N\mathbf{1}_N^T\right)\right]\otimes \mathbf{I}_2 = (L_{\sigma(t)} - 0)\otimes \mathbf{I}_2 = L_{\sigma(t)}\otimes \mathbf{I}_2.$$

Therefore, $(L_{\sigma(t)}\otimes \mathbf{I}_2)\mathbf{P} = L_{\sigma(t)}\otimes \mathbf{I}_2$.

Based on the previous discussion, the following theorem is stated.

Theorem 1. *Under Assumptions 1 and 2, if a positive scalar* μ *and positive definite matrices* Q, Q_i *of appropriate dimensions exist such that for all* $i, j \in N_g$,

$$QP_iQ = \begin{bmatrix} Q_i & \mathbf{0} \\ \mathbf{0} & \mathbf{0} \end{bmatrix}, \tag{3.8}$$

and

$$Q_i \le \mu Q_j, \tag{3.9}$$

then the distributed error estimator, as given by Eq (3.3)*, guarantees that*

$$\lim_{t\to+\infty} e(t) = \mathbf{0}, \tag{3.10}$$

provided that the switching signal $\sigma(t)$ *satisfies the average dwell time condition*

$$\tau_{ave} \ge \frac{2\ln\mu}{\lambda_{\min,F}}, \tag{3.11}$$

where $P_i = (L_i \otimes \mathbf{I}_2)K(L_i \otimes \mathbf{I}_2)$*, and* $\lambda_{\min,F}$ *has been previously defined.*

Proof. Consider the following candidate Lyapunov function:

$$V_{\sigma(t)}(\delta) = \frac{1}{2}\delta^T P_{\sigma(t)}\delta. \tag{3.12}$$

Let $\xi = Q^{-1}\delta = [\xi_1^T, \xi_2^T, \ldots, \xi_N^T]^T$, where $\xi_i \in \mathbb{R}^2$. Consequently, for all $j \in N_g$,

$$\delta^T P_j\delta = (Q\xi)^T P_j(Q\xi) = \xi^T QP_jQ\xi = \xi^T \begin{bmatrix} Q_j & \mathbf{0} \\ \mathbf{0} & \mathbf{0} \end{bmatrix}\xi = \tilde{\xi}^T Q_j\tilde{\xi}, \tag{3.13}$$

holds following Eq (3.8) for any δ with $\tilde{\xi} = [\xi_1^T, \xi_2^T, \ldots, \xi_{n-1}^T]^T$. When $\mathcal{G}_{t_h^+} \neq \mathcal{G}_{t_h^-}$, the following relation is directly obtained from Inequality (3.9) and Eq (3.13)

$$
\begin{aligned}
2V_{\sigma(t_h^+)}(\delta(t_h^+)) &= \delta^T(t_h^+)P_{\sigma(t_h^+)}\delta(t_h^+) \\
&= (Q\xi(t_h^+))^T P_{\sigma(t_h^+)}(Q\xi(t_h^+)) \\
&= \xi^T(t_h^+)QP_{\sigma(t_h^+)}Q\xi(t_h^+) \\
&= \xi^T(t_h^+)\begin{bmatrix} Q_{\sigma(t_h^+)} & \mathbf{0} \\ \mathbf{0} & \mathbf{0} \end{bmatrix}\xi(t_h^+) \\
&= \tilde{\xi}^T(t_h^+)Q_{\sigma(t_h^+)}\tilde{\xi}(t_h^+) \\
&\le \tilde{\xi}^T(t_h^-)\mu Q_{\sigma(t_h^-)}\tilde{\xi}(t_h^-) \\
&= \mu\xi^T(t_h^-)\begin{bmatrix} Q_{\sigma(t_h^-)} & \mathbf{0} \\ \mathbf{0} & \mathbf{0} \end{bmatrix}\xi(t_h^-) \\
&= \mu\xi^T(t_h^-)QP_{\sigma(t_h^-)}Q\xi(t_h^-) \\
&= \mu\delta^T(t_h^-)P_{\sigma(t_h^-)}\delta(t_h^-) \\
&= 2\mu V_{\sigma(t_h^-)}(\delta(t_h^-)).
\end{aligned} \tag{3.14}
$$

According to [13], $\mathrm{Ker}(K) \cap \mathrm{Im}(L \otimes \mathbf{I}_2) = \{\mathbf{0}\}$ holds, so using the results of Lemma 2, this function satisfies the following bounds:

$$
\lambda_{\min,P}||\delta||^2 = \min_{i\in N_g}\{\lambda_{\min}(P_i)\}\delta^T\delta \le V_{\sigma(t)}(\delta(t)) \le \max_{i\in N_g}\{\lambda_{\max}(P_i)\}\delta^T\delta = \lambda_{\max,P}||\delta||^2. \tag{3.15}
$$

Taking the time derivative of $V_{\sigma(t)}(\delta)$ with Eq (3.7) along the trajectory of t leads to the following:

$$
\begin{aligned}
\dot{V}_{\sigma(t)}(\delta) &= -\delta^T P_{\sigma(t)}\mathbf{P}K(L_{\sigma(t)} \otimes \mathbf{I}_2)\delta \\
&= -\delta^T(L_{\sigma(t)} \otimes \mathbf{I}_2)K(L_{\sigma(t)} \otimes \mathbf{I}_2)\mathbf{P}K(L_{\sigma(t)} \otimes \mathbf{I}_2)\delta \\
&= -\delta^T(L_{\sigma(t)} \otimes \mathbf{I}_2)K(L_{\sigma(t)} \otimes \mathbf{I}_2)K(L_{\sigma(t)} \otimes \mathbf{I}_2)\delta \\
&= -\delta^T(L_{\sigma(t)} \otimes \mathbf{I}_2)(K_F)^T K_F(L_{\sigma(t)} \otimes \mathbf{I}_2)(K_F)^T K_F(L_{\sigma(t)} \otimes \mathbf{I}_2)\delta \\
&= -\delta^T(L_{\sigma(t)} \otimes \mathbf{I}_2)(K_F)^T F_{\sigma(t)}K_F(L_{\sigma(t)} \otimes \mathbf{I}_2)\delta \\
&\le -\lambda_{\min}(F_{\sigma(t)})\delta^T(L_{\sigma(t)} \otimes \mathbf{I}_2)(K_F)^T K_F(L_{\sigma(t)} \otimes \mathbf{I}_2)\delta \\
&= -\lambda_{\min}(F_{\sigma(t)})\delta^T(L_{\sigma(t)} \otimes \mathbf{I}_2)K(L_{\sigma(t)} \otimes \mathbf{I}_2)\delta \\
&= -\lambda_{\min}(F_{\sigma(t)})\delta^T P_{\sigma(t)}\delta \\
&= -\lambda_{\min}(F_{\sigma(t)})V_{\sigma(t)}(\delta) \\
&\le -\lambda_{\min,F}V_{\sigma(t)}(\delta).
\end{aligned} \tag{3.16}
$$

Combining Inequalities (3.14) and (3.16), for any $t \in [t_h, t_{h+1})$, the following inequality holds:

$$
\begin{aligned}
V_{\sigma(t)}(\delta(t)) &\le exp(-\lambda_{\min,F}(t - t_h))V_{\sigma(t_h^+)}(\delta(t_h^+)) \\
&\le exp(-\lambda_{\min,F}(t - t_h))\mu V_{\sigma(t_h^-)}(\delta(t_h^-)) \\
&= exp(-\lambda_{\min,F}(t - t_h) + \ln\mu)V_{\sigma(t_h^-)}(\delta(t_h^-)) \\
&\cdots \\
&\le exp(-\lambda_{\min,F}(t - t_1) + N_\sigma(t, t_1)\ln\mu)V_{\sigma(t_1^-)}(\delta(t_1^-)) \\
&\le exp(-\lambda_{\min,F}(t - t_0) + N_\sigma(t, t_1)\ln\mu)V_{\sigma(t_0^+)}(\delta(t_0^+)) \\
&\le exp(-\lambda_{\min,F}(t - t_0) + N_\sigma(t, t_0)\ln\mu)V_{\sigma(t_0)}(\delta(t_0)),
\end{aligned} \tag{3.17}
$$

where $exp(\cdot)$ denotes the exponential operator. Since $N_\sigma(t,t_0) \le \frac{t-t_0}{\tau_{ave}}$ and Inequality (3.11) holds, the following inequality follows:

$$-\lambda_{\min,F}(t-t_0)+N_\sigma(t,t_0)\ln\mu \le -\lambda_{\min,F}(t-t_0)+\ln\mu\frac{t-t_0}{\tau_{ave}} \le -\lambda_{\min,F}(t-t_0)+\frac{\lambda_{\min,F}}{2}(t-t_0) = -\frac{\lambda_{\min,F}}{2}(t-t_0).$$

Inserting the above expression into Inequality (3.17) results in the following:

$$V_{\sigma(t)}(\delta(t)) \le exp\left(-\frac{\lambda_{\min,F}}{2}(t-t_0)\right)V_{\sigma(t_0)}(\delta(t_0)).$$

From the above inequality and Inequality (3.15), it can be concluded that

$$\|\delta(t)\| \le \kappa e^{-\alpha(t-t_0)}\|\delta(t_0)\|,\ \kappa = \sqrt{\lambda_{\max,P}/\lambda_{\min,P}},\ \alpha = \lambda_{\min,F}/4. \tag{3.18}$$

Consequently, the state $\delta(t)$ converges to zero, that is, $\lim_{t\to+\infty}\delta(t) = \mathbf{0}$. This implies that the difference between any two components of the state also converges to zero (i.e., $\lim_{t\to+\infty}(\delta_i(t)-\delta_j(t))$). Then, Eq (3.6) provides the following:

$$\lim_{t\to+\infty}(e_i(t)-e_j(t)) = \lim_{t\to+\infty}(\delta_i(t)-\delta_j(t)) = \mathbf{0}.$$

On the other hand, since $e_1(t)$ is always parallel to vector $\overrightarrow{p_1q}$ and $e_2(t)$ is always parallel to vector $\overrightarrow{p_2q}$, and given by Assumption 2 that $\overrightarrow{p_1q}$ and $\overrightarrow{p_2q}$ are not parallel, it follows that as $t\to\infty$, $e_1(t)\to 0$ and $e_2(t)\to 0$. Therefore, as $t\to\infty$, for all i, $e_i(t)\to 0$, thus proving Eq (3.10). □

The above theorem relies on the minimal-information framework of [13], which only assumes that the leaders can sense bearings or visually lock onto the target (i.e., detect its presence within their fields of view), without requiring range radar or precise absolute position measurements. Therefore, the resulting sensor suite is simple and low-cost. The necessity of Assumption 1 is straightforward. If the lines of sight of the two leaders satisfy $\theta_1 = \theta_2$ or $\theta_1 = \theta_2 \pm \pi$, that is, if the two rays are parallel or anti-parallel, then they cannot uniquely determine the target position through their intersection. In this case, even if the distributed error estimator reaches consensus, it converges to a point on an indeterminate line, thus rendering the estimation algorithm mathematically incapable of accurately localizing the target. When $|\Delta\theta| = |\theta_1-\theta_2|$ is nonzero but approaches zero, theoretical convergence still holds. However, by Lemma 1, $\lambda_{\min,F} \le C_{\min}\sin^2(\Delta\theta)$, and therefore $\lambda_{\min,F}\to 0$ as $\Delta\theta\to 0$, thus causing the estimation error to decay arbitrarily slowly. Hence, in practical deployments, $\Delta\theta$ should remain sufficiently far from 0 and π. Typically, it is advisable to impose a safety threshold, such as $\Delta\theta \ge 15^\circ$.

Remark 4. *Note that*

$$\|e_1(t)-e_2(t)\| = \|\delta_1(t)-\delta_2(t)\| \le \|\delta_1(t)\| + \|\delta_2(t)\| \le \sqrt{2(\|\delta_1(t)\|^2+\|\delta_2(t)\|^2)} \le \sqrt{2}\|\delta(t)\|,$$

and

$$\|e_1(t)-e_2(t)\|^2 = \|e_1(t)\|^2 + \|e_2(t)\|^2 - 2\|e_1(t)\|\|e_2(t)\|\cos\Delta\theta \ge (\|e_1(t)\| + \|e_2(t)\|)^2\sin^2(\Delta\theta/2).$$

Given $\Delta\theta \ge 15^\circ$*, it follows* $\sin(\Delta\theta/2) \ge \sin(7.5^\circ)$ *and*

$$\|e_1(t)\| + \|e_2(t)\| \le \|e_1(t)-e_2(t)\|/\sin(7.5^\circ) \le \sqrt{2}\|\delta(t)\|/\sin(7.5^\circ).$$

According to $e_i(t) = \delta_i(t) + \bar{e}(t)$, applying the triangle inequality yields

$$\|\bar{e}(t)\| = \|e_1(t) - \delta_1(t)\| \leq \|e_1(t)\| + \|\delta_1(t)\|$$

and

$$\|\bar{e}(t)\| = \|e_2(t) - \delta_2(t)\| \leq \|e_2(t)\| + \|\delta_2(t)\|.$$

Summing these two inequalities gives

$$2\|\bar{e}(t)\| \leq \|e_1(t)\| + \|e_2(t)\| + \|\delta_1(t)\| + \|\delta_2(t)\| \leq \sqrt{2}\|\delta(t)\|/\sin(7.5^\circ) + \sqrt{2}\|\delta(t)\|,$$

which implies that $\|\bar{e}(t)\| \leq \overline{C}\|\delta(t)\|$, where $\overline{C} = (1 + \sin(7.5^\circ))/(\sqrt{2}\sin(7.5^\circ))$. On the other hand,

$$\|e(t)\|^2 = \|\delta(t)\|^2 + \|(\mathbf{1}_N \otimes \mathbf{I}_2)\bar{e}(t)\|^2 + 2\delta(t)^T(\mathbf{1}_N \otimes \mathbf{I}_2)\bar{e}(t) = \|\delta(t)\|^2 + N\|\bar{e}(t)\|^2,$$

which implies

$$\|e(t)\| = \sqrt{\|\delta(t)\|^2 + N\|\bar{e}(t)\|^2} \leq \|\delta(t)\| + \sqrt{N}\|\bar{e}(t)\|.$$

In summary, $\|e(t)\| \leq K\left(1 + \overline{C}\sqrt{N}\right)e^{-\alpha(t-t_0)}\|e(t_0)\|$. Consequently, for a given continuous time interval $[t_0, t_0 + T]$ and a boundary threshold $c_1 > 0$, if the initial condition satisfies $\|e(t_0)\| \leq c_1$, the system state guarantees finite-time boundedness such that $\|e(t)\| \leq c_2$ for all $t \in [t_0, t_0 + T]$, where $c_2 = K\left(1 + \overline{C}\sqrt{N}\right)c_1$. Finite-time or fixed-time consensus control strategies, such as those in [21, 22], typically rely on non-smooth feedback or fractional-power dynamics to achieve convergence within a finite or prescribed time horizon. However, in our formulation, the geometric constraints imposed by the semi-positive definite matrices make it difficult to prove exact zero convergence in finite or fixed time within the present analysis. Therefore, the present result establishes finite-time boundedness over a specified interval, rather than exact finite-time or fixed-time convergence to the origin.

Remark 5. *From Reference [13], it is known that rank$(P) = r_P > 0$. Since $P \geq 0$, there exists a matrix $U = [U_1, U_2]$ such that $P = U^T U$, where $U_1 \in \mathbb{R}^{r_P \times r_P}$ is invertible and $U_2 \in \mathbb{R}^{r_P \times (2N - r_P)}$. Let $W = -U_1^{-1}U_2 \in \mathbb{R}^{r_P \times (2N - r_P)}$. For arbitrary positive definite matrices $A \in \mathbb{R}^{r_P \times r_P}$ and $C \in \mathbb{R}^{(2N - r_P) \times (2N - r_P)}$, the equality $QPQ = \begin{bmatrix} A^T U_1^T U_1 A & 0 \\ 0 & 0 \end{bmatrix} \geq 0$ holds, where $Q = \begin{bmatrix} A + WCW^T & WC \\ CW^T & C \end{bmatrix} > 0$, and $A^T U_1^T U_1 A > 0$. It is evident that the positive definite matrix $Q \in \mathbb{R}^{2N \times 2N}$ is not unique. For any positive definite matrix $Q^{N-1} \in \mathbb{R}^{N-1 \times N-1}$ and positive scalar c, if $(c - c^2 \mathbf{1}_{N-1}^T (Q^{N-1})^{-1} \mathbf{1}_{N-1}) \otimes \mathbf{I}_2$ is also positive definite, then*

$$Q = \begin{bmatrix} Q^{N-1} & c\mathbf{1}_{N-1} \\ c\mathbf{1}_{N-1}^T & c \end{bmatrix} \otimes \mathbf{I}_2 \tag{3.19}$$

is a candidate matrix. This is because Eq (3.8) holds if and only if both $QP_iQ([0, ..., 0, 1]^T \otimes \mathbf{I}_2) = 0$ and $([0, ..., 0, 1] \otimes \mathbf{I}_2)QP_iQ = 0$ hold. The condition $QP_iQ([0, ..., 0, 1]^T \otimes \mathbf{I}_2) = 0$ implies that $P_iQ([0, ..., 0, 1]^T \otimes \mathbf{I}_2) = 0$, which, in turn, yields $(L_i \otimes \mathbf{I}_2)K(L_i \otimes \mathbf{I}_2)Q([0, ..., 0, 1]^T \otimes \mathbf{I}_2) = 0$. Combining this with Lemma 1 indicates that $(L_i \otimes \mathbf{I}_2)Q([0, ..., 0, 1]^T \otimes \mathbf{I}_2) = 0$, i.e.,

$$Q([0, ..., 0, 1]^T \otimes \mathbf{I}_2) = \left(\begin{bmatrix} Q^{N-1} & c\mathbf{1}_{N-1} \\ c\mathbf{1}_{N-1}^T & c \end{bmatrix}[0, ..., 0, 1]^T\right) \otimes \mathbf{I}_2 = \begin{bmatrix} c\mathbf{1}_{N-1} \\ c \end{bmatrix} \otimes \mathbf{I}_2.$$

Similarly,

$$([0,...,0,1]\otimes \mathbf{I}_2) * Q = \left([0,...,0,1]\begin{bmatrix} Q^{N-1} & c\mathbf{1}_{N-1} \\ c\mathbf{1}_{N-1}^T & c \end{bmatrix}\right)\otimes \mathbf{I}_2 = \begin{bmatrix} c\mathbf{1}_{N-1}^T c \end{bmatrix}\otimes \mathbf{I}_2.$$

Therefore, $Q = \begin{bmatrix} k\mathbf{I}_{N-1} & c\mathbf{1}_{N-1} \\ c\mathbf{1}_{N-1}^T & c \end{bmatrix}\otimes \mathbf{I}_2$ *is a special case of Eq* (3.19) *if* $k > c(N-1) > 0$*, which must satisfy Eq* (3.8).

Based on the above remark, Algorithm 1 is proposed for applying Theorem 1.

Algorithm 1: Computation of the minimum admissible average dwell time.

Input: Leader angles θ_1, θ_2; Number of agents/topologies N/g; Graph Laplacians $L_1, L_2, \ldots, L_g$.

Precomputation:

Construct $K_F = \text{bkdg}\{[\cos\theta_1 \sin\theta_1], [\cos\theta_2 \sin\theta_2], \underbrace{\mathbf{I}_2, \ldots, \mathbf{I}_2}_{N-2}\}$, and set $K = K_F^T K_F$;

Compute $\lambda_{\min,F} = \min\limits_{i\in\{1,\ldots,g\}} \{\lambda_{\min}(K_F(L_i \otimes \mathbf{I}_2)K_F^T)\}$.

LMI optimization:

Choose parameters k, c; Construct $Q = \begin{bmatrix} k\mathbf{I}_{N-1} & c\mathbf{1}_{N-1} \\ c\mathbf{1}_{N-1}^T & c \end{bmatrix}\otimes \mathbf{I}_2$;

For $i = 1, \ldots, g$, define Q_i as the upper-left block of QP_iQ, i.e., $QP_iQ = \begin{bmatrix} Q_i & \mathbf{0} \\ \mathbf{0} & \mathbf{0} \end{bmatrix}$;

Solve the optimization problem: $\begin{cases} \min \mu \\ \text{subject to} \begin{cases} Q_i \le \mu Q_j, \ i \ne j; \\ 0 < \mu; \end{cases} \end{cases}$

if infeasible

terminate (no admissible τ_{ave} exists);

else

set $\mu^* = \min \mu$;

end

Then, one may choose $\tau_{ave} \ge 2\ln\mu^*/\lambda_{\min,F}$ to guarantee stability.

Inequalities (3.8) and (3.9) in Theorem 1 are used to establish Inequality (3.14), which can be replaced by an easier condition to achieve the same function as follows:

$$\lambda_{\max}(P_j) \le \mu\, \lambda_{\min}^{+}(P_i). \tag{3.20}$$

Based on this, the following corollary obviously follows Theorem 1.

Corollary 1. *Under Assumptions 1 and 2, if a positive scalar* μ *exists such that for all* $i, j \in N_g$*, and Inequality* (3.20) *holds, then the distributed error estimator, given by Eq* (3.3)*, guarantees that Eq* (3.10) *holds, provided that the switching signal* $\sigma(t)$ *satisfies the average dwell time condition described by Inequality* (3.11)*, where all symbols are defined in the preceding text.*

Proof. Consider the same candidate Lyapunov function as Eq (3.12). It is straightforward to derive from Inequality (3.20) that

$$\begin{aligned}
V_{\sigma(t_h^+)}(\delta(t_h^+)) &= \frac{1}{2}\delta^T(t_h^+)P_{\sigma(t_h^+)}\delta(t_h^+) \\
&\leq \frac{1}{2}\delta^T(t_h^+)\lambda_{\max}(P_{\sigma(t_h^+)})\delta(t_h^+) \\
&\leq \frac{1}{2}\delta^T(t_h^-)\mu\,\lambda_{\min}^+(P_{\sigma(t_h^-)})\delta(t_h^-) \\
&\leq \frac{1}{2}\delta^T(t_h^-)\mu P_{\sigma(t_h^-)}\delta(t_h^-) \\
&= \mu V_{\sigma(t_h^-)}(\delta(t_h^-)).
\end{aligned}$$

Then, similarly to the proof of Theorem 1, the proof ends. □

The convergence of the distributed error estimator, as given by Eq (3.3), validates the convergence and effectiveness of the distributed relative position estimator, as given by Eq (3.2). Subsequently, this estimator, formulated in Eq (3.2), enables the cooperative pointing control of the system described by Eq (2.1), thereby driving the orientation angles to follow the local control input u_i as follows:

$$u_i(t) \equiv 0,\ i = 1, 2, \tag{3.21a}$$

$$u_i(t) = \begin{cases} 0, & \text{if } \|\hat{d}_i(t)\| = 0 \\ -k(\theta_i(t) - \hat{\theta}_i(t)), & \text{otherwise} \end{cases},\ i = 3, 4, \ldots, N, \tag{3.21b}$$

where $k > 0$, $r > 0$,

$$\hat{\theta}_i = (1 - s_i)\pi + s_i \arccos\left(\frac{[1, 0]\hat{d}_i}{\|\hat{d}_i\|}\right),$$

$s_i = \operatorname{sgn}\left(\operatorname{sgn}([1, 0]\hat{d}_i) + 0.5\right)$, and $\hat{d}_i$ is the solution to Eq (3.2). It is easy to know that $\hat{\theta}_i \in [0, 2\pi)$ and $s_i = \begin{cases} 1, & \text{if } [0, 1]\hat{d}_i \geq 0 \\ -1, & \text{otherwise} \end{cases}$.

Then, the main result for the cooperative pointing control of the system, formulated in Eq (2.1), is presented in the following theorem.

Theorem 2. *Under Assumptions 1 to 2 and Theorem 1, if the time-varying communication topology graph $\mathcal{G}_t$ satisfies the average dwell time condition in Eq* (3.11)*, then the cooperative pointing control given by Eq* (3.21) *works for the system described by Eq* (2.1)*, namely $\theta_i(t) \to \theta_i^*$ as $t \to \infty$.*

Proof. By Theorem 1, there hold $\lim_{t\to\infty} \hat{d}_i(t) = d_i$ and $\lim_{t\to\infty} \hat{\theta}_i(t) = \theta_i^*$, for $i = 3, 4, \ldots, N$. For any $r > 0$, there exist $T > 0$ such that $\|\hat{d}_i(t) - d_i\| < r$ for all $i = 3, \ldots, N$ and all $t > T$. Then, for a sufficiently small $r_\varepsilon > 0$, there exist $T_\varepsilon > 0$ such that $\|\hat{d}_i(t)\| \in [\|d_i\| - r, \|d_i\| + r]$ for all $i = 3, \ldots, N$ and all $t > T_\varepsilon$, which implies that $\|\hat{d}_i(t)\| \neq 0$ for all $i = 3, \ldots, N$ and all $t > T_\varepsilon$. At this time, Eq (3.21b) degenerates into the following:

$$u_i(t) = -k(\theta_i(t) - \hat{\theta}_i(t)),\ i = 3, 4, \ldots, N.$$

Define $\bar{\theta}_i(t) := \theta_i(t) - \theta_i^*$, $\bar{\hat{\theta}}_i(t) := \hat{\theta}_i(t) - \theta_i^*$. From Eqs (2.1) and (3.21), it follows that

$$\dot{\bar{\theta}}_i = -k(\bar{\theta}_i - \bar{\hat{\theta}}_i).$$

Since $\bar{\bar{\theta}}_i(t) \to 0$ as $t \to \infty$, the application of the ISS theorem yields $\bar{\theta}_i(t) \to 0$ as $t \to \infty$ (i.e., $\theta_i(t) \to \theta^*$ as $t \to \infty$). This completes the proof. □

Table 1. Comparison of cooperative pointing control approaches.

Index	Metric (Quantitative indicators)	Ours	[8]	[9]	[10]	[11]	[12]	[13]
1	Leaders with target detection	**2**	2	2	2	4	0[‡1]	**2**
2	Exteroceptive sensors per non-leader	**0**	≥ 1	≥ 1	≥ 1	≥ 1	≥ 1	**0**
3	Absolute global coordinates (p_i) needed?	**No**	Yes	Yes	Yes	Yes	Yes	Yes
4	Number of neighbors per non-leader	n_i	2	2	2	≤ 4	n_i	n_i
5	Data load per non-leader (floats)	$2n_i$	4	6	6+	8	$\geq 3n_i$	$2n_i$
6	Communication scaling (w.r.t. N)[‡2]	$O(1)$	$O(1)$	$O(1)$	$O(1)$	$O(1)$	$O(n_i)$	$O(1)$
7	Trig. ops per non-leader per iteration	**1**	≥ 9	≥ 3	≥ 5	> 10	0	≥ 1
8	Case-by-case geometry redesign needed?	**No**	Yes	Yes	Yes	Yes	Yes	**No**
9	Non-leader deployment freedom	2D (arbitrary)	1D (line)	1D (line)	1D (line)	2D (plane)	3D (space)	2D (arbitrary)

‡1 [12] achieves 0 leaders only because its target is strictly fixed as the weighted centroid (Fermat-Weber point) of the agents' positions.

‡2 $O(1)$ with respect to N signifies that the per-node load remains constant under a bounded neighbor degree (a standard assumption in wireless networks; applicable to our method and [8–11]). Crucially, the target in [12] is the dynamic Fermat–Weber centroid of all agents, not a fixed external target. Consequently, their load inherently scales with n_i and cannot be bounded by a constant independent of N.

Remark 6. *Before presenting the numerical simulations, Table 1 compares the proposed method with existing cooperative pointing control schemes [8–13]. In [8–12], each non-leader agent requires at least one exteroceptive sensor (Row 2: '≥ 1') to measure the neighbors' geometric or bearing information (positions, angles, or bearing vectors) for control-law computations. Contrastingly, our method and [13] only require two leaders with target detection capability, while non-leaders do not need exteroceptive sensors (Row 2: '0'), solely relying on communication and proprioception. This reduction in sensing requirements arises from our estimator-pointing separation framework, which concentrates sensing tasks on a few leaders, thereby freeing the majority of agents from exteroceptive hardware. Regarding communication and the computational burden, our method and [13] only exchange $2n_i$ floats per non-leader per iteration (Row 5), thus yielding $O(1)$ communication scaling with respect to N for bounded-degree graphs (Row 6). Computationally, our method only requires one trigonometric operation per non-leader per iteration (Row 7), which is the lowest cost among methods supporting arbitrary planar deployment. Although [8] achieves a communication load of 4 floats, it requires ≥ 9 trigonometric operations and is limited to 1D collinear deployments. Likewise, [9] and [10] require 6 and 6+ floats, respectively, with ≥ 3 and ≥ 5 trigonometric operations per iteration, while sharing the same 1D limitation. [11] supports 2D planar deployment, but at the cost of 8 floats and > 10 trigonometric operations per iteration, giving it the highest computational burden among the compared methods. [12] reports 0 trigonometric operations, but requires 3D projection matrices per neighbor, as well as power operations, both of which are computationally more demanding than scalar trigonometric evaluations. Furthermore, its communication load of ≥ $3n_i$ floats scales with n_i and cannot be bounded independently of N (Row 6:*

$O(n_i)$). [13] shares our advantages in communication and sensing when the switching estimator is inactive. Moreover, [8–11] require case-by-case geometric redesign for each deployment change (Row 8: 'Yes') (e.g., from collinear to planar or from 2D to 3D). In contrast, our estimator-pointing separation framework unifies arbitrary planar deployments without requiring geometric relationships to be re-derived ('No' in Row 8). Additionally, it supports time-varying topologies and eliminates the need for global absolute coordinates, making it highly scalable in dynamic, GPS-denied environments. In summary, our method achieves lower sensing requirements and greater implementation flexibility than the compared approaches.

4. Numerical simulation

This section verifies the feasibility and effectiveness of the proposed distributed relative position estimator. First, consider a set of 10 coplanar agents is considered, with connected undirected graphs switching between $\mathcal{G}_1$ and $\mathcal{G}_2$, illustrated in Figure 2 to describe the communication topologies among the above 10 agents and known conditions provided in the ITEM1, VALUE 1, ITEM2, VALUE 2, ITEM3, and VALUE 3 columns of Table 2.

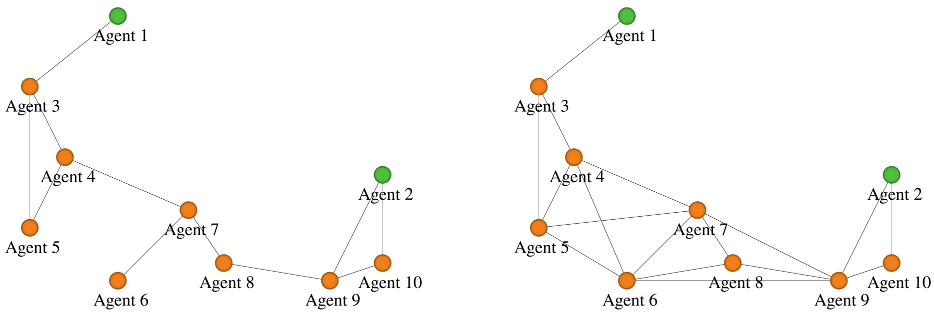

(a) The diagram of $\mathcal{G}_1$ **(b)** The diagram of $\mathcal{G}_2$.

Figure 2. The diagram of communication topologies.

Table 2. Known conditions and initial conditions.

ITEM 1	VALUE 1	ITEM 2	VALUE 2	ITEM 3	VALUE 3	ITEM 4	VALUE 4	ITEM 5	VALUE 5
θ_1	$0°$	$d_{1,3}$	$[-5,-4]^T$	$d_{4,7}$	$[\ 7,-3]^T$	$d_{7,9}$	$[\ 8,-4]^T$	t_0	0s
θ_2	$90°$	$d_{3,4}$	$[\ 2,-4]^T$	$d_{5,6}$	$[\ 5,-3]^T$	$d_{8,9}$	$[\ 6,-1]^T$	$\hat{d}_1(t_0)$	$[2,0]^T$
		$d_{3,5}$	$[\ 0,-8]^T$	$d_{6,7}$	$[\ 4,\ \ 4]^T$	$d_{9,10}$	$[\ 3,\ \ 1]^T$	$\hat{d}_2(t_0)$	$[0,2]^T$
		$d_{4,5}$	$[-2,-4]^T$	$d_{6,8}$	$[\ 6,\ \ 1]^T$	$d_{9,2}$	$[\ 3,\ \ 6]^T$	$\hat{d}_i(t_0), i \neq 1,2$	$[1,1]^T$
		$d_{4,6}$	$[\ 3,-7]^T$	$d_{7,8}$	$[\ 2,-3]^T$	$d_{10,2}$	$[\ 0,\ \ 5]^T$		

By setting $c = 1$ and $k = 10$ satisfying Eq (3.8), and applying the MATLAB R2025a LMI toolbox to solve the linear matrix inequality described in Eq (3.9), $\mu = 1.737362$ is obtained. Under the topologies $\mathcal{G}_1$ and $\mathcal{G}_2$, with $\mu = 1.74$ and $\lambda_{\min,F} = 0.0436$ computed, the ratio $2\mu/\lambda_{\min,F}$ yields 79.8165. The switching signals $\sigma_1(t)$ and $\sigma_2(t)$ are chosen as follows:

$$\sigma_1(t) = \begin{cases} 1, & \text{if } t \in [160k, 160k+20), k = 0, 1, 2, \dots \\ 2, & \text{otherwise} \end{cases},$$

$$\sigma_2(t) = \begin{cases} 2, & \text{if } t \in [160k, 160k+20), k = 0, 1, 2, \dots \\ 1, & \text{otherwise} \end{cases},$$

with $\tau_{ave} = 80 > 79.670462$, where $\sigma_1(t)$ denotes that $\mathcal{G}_1$ has a longer dwell time than $\mathcal{G}_2$, and $\sigma_2(t)$ denotes that $\mathcal{G}_2$ has a longer dwell time than $\mathcal{G}_1$.

First, consider the switching signal $\sigma_1(t)$. With the initial conditions $\hat{d}(t_0)$ given in Table 2, which satisfies Assumption 2, the trajectory of d over [0, 150 s) is shown in Figure 3. The curves demonstrate that each component of $\hat{d}$ converges under the distributed relative position estimator in Eq (3.2), where $\hat{d}_i = [\hat{d}_{i,x}, \hat{d}_{i,y}]$. Specially, for Agents 1 and 2, the $\hat{d}_{1,y}$ and $\hat{d}_{2,x}$ components remain unchanged, which indicates the role of the projection matrix, which ensures that the leaders' line of sight to the target does not deviate. Furthermore, the starting points of $\hat{d}_i$, $i = 1, 2, \dots, 10$ are aligned with the corresponding p_i at $t = 5s, 20s, 150s$, as depicted in Figure 4. In Figure 4, the red origin represents the target, the green origins represent the leaders (Agents 1 and 2), the orange origins represent the non-leader agents (Agents 3 to 10), and the green and orange lines represent the relative position estimates $\hat{d}_1$, $\hat{d}_2$, and $\hat{d}_3$ to $\hat{d}_{10}$, respectively. Figure 3 shows the convergence of $\hat{d}$, while Figure 4 clearly illustrates this convergence that the estimated distances approach the relative distances between each agent and the target.

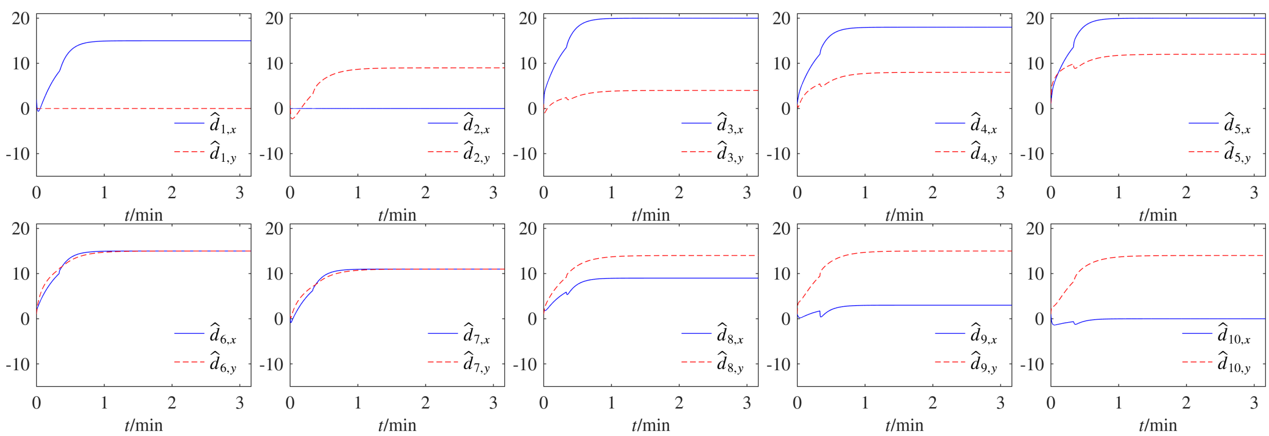

Figure 3. The trajectory of $\hat{d}$ over [0, 150 s) under switching signal $\sigma_1(t)$.

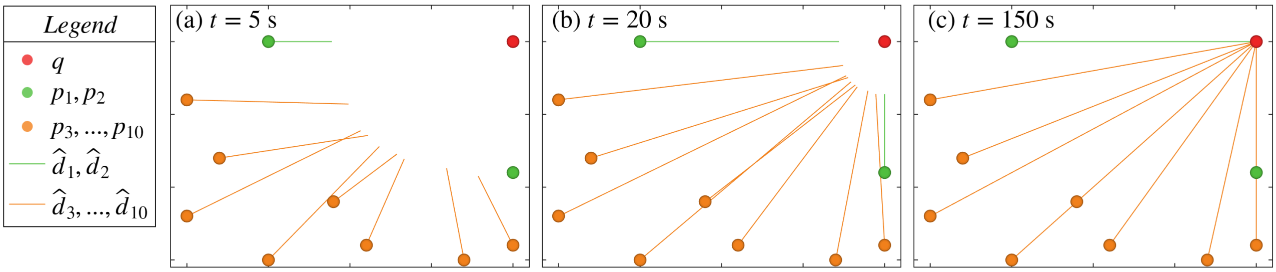

Figure 4. The diagram of $\hat{d}$ at t=5 s, 20 s, 150 s.

The errors $\{e_i\}_{i=1}^N$ and the orientation differences $\{\Delta\theta_i\}_{i=1}^N$ under the switching signals $\sigma_1(t)$ and $\sigma_2(t)$ are shown in Figures 5 and 6, respectively, where $e_i = [e_{i,x}, e_{i,y}]$, and $\Delta\theta_i = \theta_i - \theta_i^*$. The trajectories, almost converging to zero in 3 minutes, are visible in the figures. These convergence curves show that different switching signals only affect the convergence trajectory and rate, without changing the convergence trend or the fact that the signals converge to zero, which, in turn, demonstrates the effectiveness of the control protocol in Eq (3.21) driven by the relative-position-dependent distributed relative position estimator described in Eq (3.2). It should be emphasized that although the computation of $\{e_i\}_{i=1}^N$ and $\{\Delta\theta_i\}_{i=1}^N$ requires the global absolute coordinates of the agents and the target, this computation and the corresponding trajectory plots are solely presented to illustrate the convergence time. The actual state trajectory of the estimator, as shown in Figure 3, still does not require the global absolute coordinates of the agents and the target.

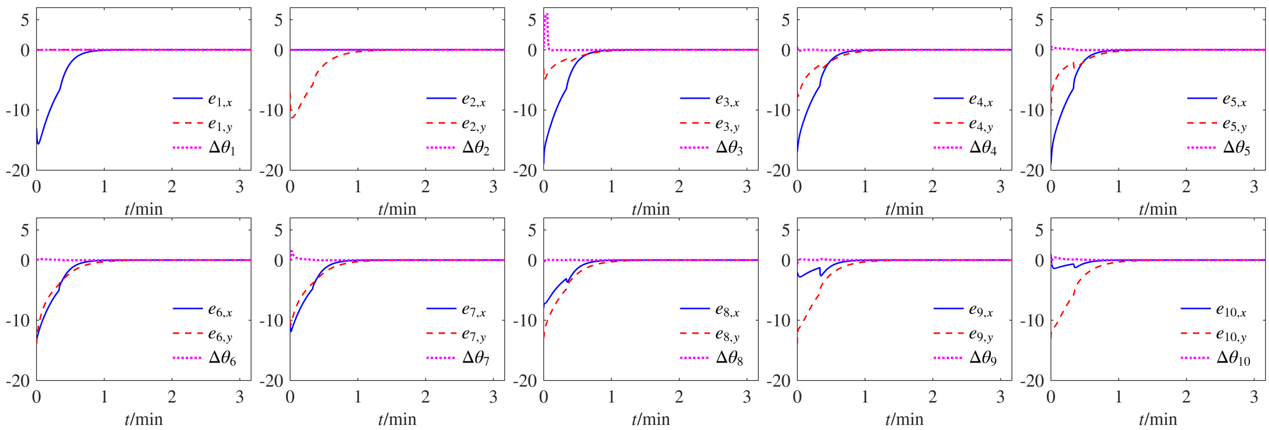

Figure 5. The trajectory of e and θ over [0, 150 s) under switching signal $\sigma_1(t)$.

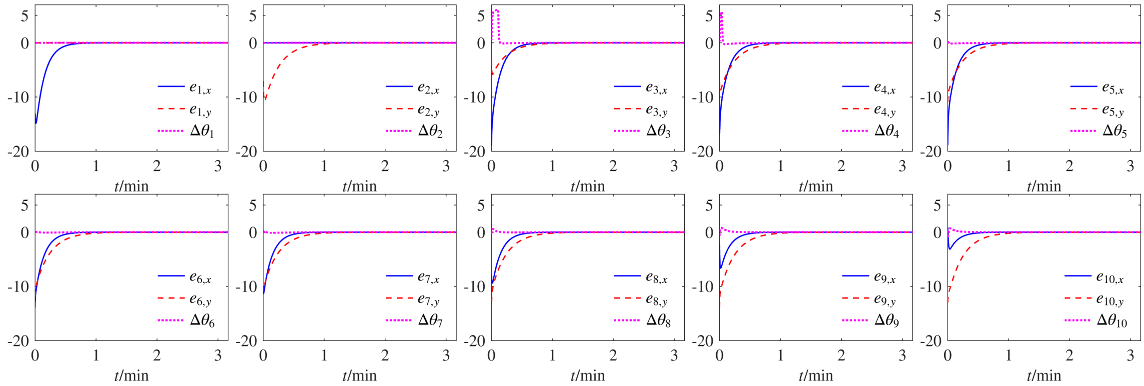

Figure 6. The trajectory of e and θ over [0, 150 s) under switching signal $\sigma_2(t)$.

Furthermore, consider the error $\|e\|$ under the six cases shown in Figure 7, where the topology does not switch. In these cases, the leaders and the target remain unchanged, with $\hat{d}_1(t_0) = [2, 0]^T$, $\hat{d}_2(t_0) = [0, 2]^T$ and $\hat{d}_i(t_0) = [1, 1]^T$ for $i \neq 1, 2$. Figure 7(a),(d) correspond to a 10-node network, Figure 7(b),(e) correspond to a 30-node network, and Figure 7(c),(f) correspond to a 40-node network. Figure 7(a)–(c) represent the minimally connected cases, while Figure 7(d)–(f) represent the maximally connected cases in which the leaders are not directly connected. The simulation results in Figure 8 indicate that, for the same node layout, $\|e\|$ converges faster on denser communication graphs than on sparser ones. Moreover, although the convergence rate of $\|e\|$ decreases with the number of nodes, it still converges to nearly zero within 20 minutes, even in the minimally connected case. These results suggest that the proposed cooperative control method has potential for applications in large-scale multi-agent systems.

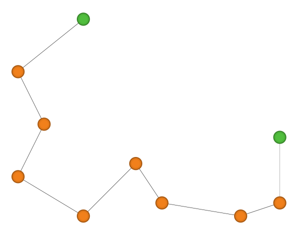

(a) The diagram of $\mathcal{G}_3$

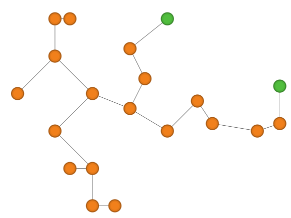

(b) The diagram of $\mathcal{G}_4$.

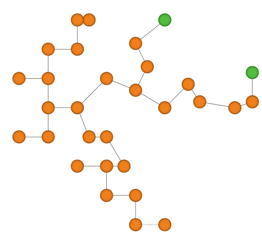

(c) The diagram of $\mathcal{G}_5$.

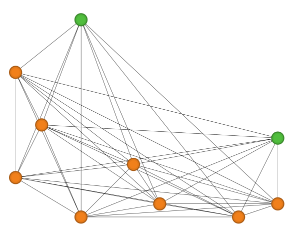

(d) The diagram of $\mathcal{G}_6$.

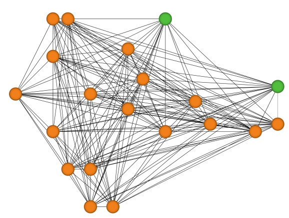

(e) The diagram of $\mathcal{G}_7$.

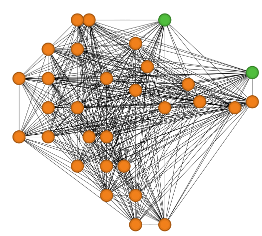

(f) The diagram of $\mathcal{G}_8$.

Figure 7. The diagram of communication topologies.

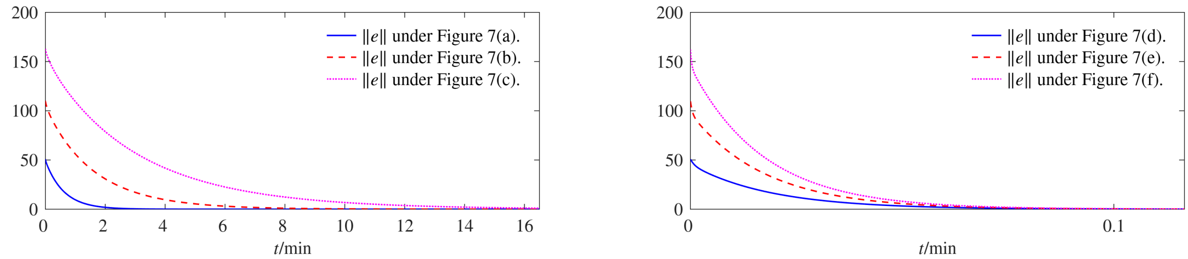

(a) The trajectory of e under $\mathcal{G}_3 - \mathcal{G}_5$.

(b) The trajectory of e under $\mathcal{G}_6 - \mathcal{G}_8$.

Figure 8. The trajectory of e under the communication graphs in Figure 7.

5. Conclusions

This paper proposed a cooperative control protocol that depends on relative position. It is designed for stationary multi-agent systems to point cooperatively toward a fixed target under switching communication topologies. The orientation-angle information is applied to combine target localization with local pointing control. A projection-matrix-based estimator and local control laws guarantee asymptotic convergence. For the convergence analysis, an error estimator and multiple Lyapunov functions are designed to explicitly handle the positive semidefinite projection matrices and the switching topologies. While the proposed protocol has demonstrated effectiveness in simulations, the current study, conducted under an idealized setting, does not account for initialization errors, communication delays, packet losses, or localization uncertainties. Improving the protocol's robustness under these non-ideal factors will be essential for experimental validation on real robotic or UAV platforms, and this will be addressed in our future work.

Use of AI tools declaration

The authors declare they have not used Artificial Intelligence (AI) tools in the creation of this article.

Acknowledgments

This work was partially supported by the National Natural Science Foundation of China under Grants 62403100 and 62473071, the National Key R&D Program of China under Grant 2023YFB3307101, the Natural Science Foundation of Liaoning Province under Grant 2024-BSBA-07, and the Fundamental Research Funds for the Central Universities under Grants 3132026107 and 3132026194.

Conflict of interest

Bing Tan is a special issue editor of Electronic Research Archive and was not involved in the editorial review or the decision to publish this article. All authors declare that there are no competing interests.

References

1. J. Yin, Y. H. Li, S. K. Liao, M. Yang, Y. Cao, L. Zhang, et al., Entanglement-based secure quantum cryptography over 1120 kilometres, *Nature*, **582** (2020), 501–505. https://doi.org/10.1038/s41586-020-2401-y
2. G. Dubus, J. L. Contreras, S. Funk, Y. Gallant, T. Hassan, J. Hinton, et al., Surveys with the Cherenkov telescope array, *Astropart. Phys.*, **43** (2013), 317–330. https://doi.org/10.1016/j.astropartphys.2012.05.020
3. S. Nag, C. K. Gatebe, D. W. Miller, O. L. De Weck, Effect of satellite formations and imaging modes on global albedo estimation, *Acta Astronaut.*, **126** (2016), 77–97. https://doi.org/10.1016/j.actaastro.2016.04.004
4. D. Wang, Q. Pan, C. Zhao, J. Hu, Z. Xu, F. Yang, et al., A study on camera array and its applications, *IFAC-PapersOnLine*, **50** (2017), 10323–10328. https://doi.org/10.1016/j.ifacol.2017.08.1662
5. R. J. A. A. Nathan, I. Kurmi, O. Bimber, Drone swarm strategy for the detection and tracking of occluded targets in complex environments, *Commun. Eng.*, **2** (2023), 55. https://doi.org/10.1038/s44172-023-00104-0
6. H. Bai, M. Arcak, J. T. Wen, Rigid body attitude coordination without inertial frame information, *Automatica*, **44** (2008), 3170–3175. https://doi.org/10.1016/j.automatica.2008.05.018
7. D. V. Dimarogonas, P. Tsiotras, K. J. Kyriakopoulos, Leader-follower cooperative attitude control of multiple rigid bodies, *Syst. Control Lett.*, **58** (2009), 429–435. https://doi.org/10.1016/j.sysconle.2009.02.002
8. F. Zhang, P. Ramazi, M. Cao, Distributed concurrent targeting for linear arrays of point sources, *IFAC Proc. Vol.*, **47** (2014), 8323–8328. https://doi.org/10.3182/20140824-6-ZA-1003.02325
9. J. Wu, W. Pu, F. Zhang, W. Yu, Decentralized targeting control of collinear agents, *Asian J. Control*, **24** (2022), 782–793. https://doi.org/10.1002/asjc.2656
10. J. Wu, S. Yuan, Q. Dang, F. Zhang, W. Yu, Cooperative pointing control of collinear double-integrators without angular velocity, *J. Franklin Inst.*, **360** (2023), 9050–9064. https://doi.org/10.1016/j.jfranklin.2022.08.026
11. P. Ramazi, F. Zhang, M. Cao, Cooperative concurrent targeting for planar arrays of point sources, *Automatica*, **159** (2024), 111357. https://doi.org/10.1016/j.automatica.2023.111357
12. M. H. Trinh, D. Zelazo, H. S. Ahn, Pointing consensus and bearing-based solutions to the Fermat–Weber location problem, *IEEE Trans. Autom. Control*, **65** (2019), 2339–2354. https://doi.org/10.1109/TAC.2019.2927932
13. F. Zhang, C. L. Jin, W. Xia, X. M. Sun, H. Bai, Cooperative pointing control of multi-robot systems via distributed target estimation, *Syst. Control Lett.*, **197** (2025), 106023. https://doi.org/10.1016/j.sysconle.2025.106023
14. S. Lin, P. Dong, C. Jin, Leader-follower-based cooperative target localization for multi-agent systems, *Chin. J. Eng.*, **48** (2026), 1247–1254. https://doi.org/10.13374/j.issn2095-9389.2025.09.02.002

15. K. You, Z. Li, L. Xie, Consensus condition for linear multi-agent systems over randomly switching topologies, *Automatica*, **49** (2013), 3125–3132. https://doi.org/10.1016/j.automatica.2013.07.024

16. Y. Li, K. Yu, M. Lv, S. Tong, Asynchronous coordination for output regulation in heterogeneous nonlinear MASs with jointly connected switching topologies, *IEEE Trans. Autom. Control*, **70** (2025), 1859–1866. https://doi.org/10.1109/TAC.2024.3466872

17. B. Liu, T. Chu, L. Wang, G. Xie, Controllability of a leader-follower dynamic network with switching topology, *IEEE Trans. Autom. Control*, **53** (2008), 1009–1013. https://doi.org/10.1109/TAC.2008.919548

18. H. Xu, S. Liu, B. Wang, J. Wang, Distributed observer design over directed switching topologies, *IEEE Trans. Autom. Control*, **70** (2024), 1623–1636. https://doi.org/10.1109/TAC.2024.3462533

19. L. Ding, M. Ye, D. Yue, Communication-efficient distributed Nash equilibrium seeking under switching topologies: A decentralized gradient-based event-triggered scheme, *Automatica*, **167** (2024), 111738. https://doi.org/10.1016/j.automatica.2024.111738

20. H. Yang, Y. Wang, Finite-gain based prescribed-time consensus control for multi-agent systems under switching topology, *Automatica*, **183** (2026), 112686. https://doi.org/10.1016/j.automatica.2025.112686

21. B. Ning, Q. L. Han, Prescribed finite-time consensus tracking for multiagent systems with nonholonomic chained-form dynamics, *IEEE Trans. Autom. Control*, **64** (2019), 1686–1693. https://doi.org/10.1109/TAC.2018.2852605

22. X. Jin, Adaptive fixed-time control for MIMO nonlinear systems with asymmetric output constraints using universal barrier functions, *IEEE Trans. Autom. Control*, **64** (2019), 3046–3053. https://doi.org/10.1109/TAC.2018.2874877

AIMS Press

© 2026 the Author(s), licensee AIMS Press. This is an open access article distributed under the terms of the Creative Commons Attribution License (https://creativecommons.org/licenses/by/4.0)